ELSEVIER

Biochimica et Biophysica Acta 1459 (2000) 49–60

BIOCHIMICA ET BIOPHYSICA ACTA
BBA

www.elsevier.com/locate/bba

Molecular contacts in the transmembrane *c*-subunit oligomer of F-ATPases identified by tryptophan substitution mutagenesis

Claudia Schnick [a], Lucy R. Forrest [b], Mark S.P. Sansom [b], Georg Groth [a,*]

[a] *Heinrich-Heine-Universität Düsseldorf, Biochemie der Pflanzen, Universitätsstr. 1, 40225 Düsseldorf, Germany*

[b] *Laboratory of Molecular Biophysics, Department of Biochemistry, University of Oxford, The Rex Richards Building, South Parks Road, Oxford OX1 3QU, UK*

Received 22 November 1999; received in revised form 21 January 2000; accepted 2 March 2000

Abstract

When isolated in its monomeric form, subunit *c* of the proton transporting ATP synthase of *Escherichia coli* was shown to fold in a hairpin-like structure consisting of two hydrophobic membrane spanning helices and a short connecting hydrophilic loop. In the plasma membrane of *Escherichia coli*, however, about 9–12 *c*-subunit monomers form an oligomeric complex that functions in transmembrane proton conduction and in energy transduction to the catalytic F_1 domain. The arrangement of the monomers and the molecular architecture of the complex were studied by tryptophan scanning mutagenesis and restrained MD simulations. Residues 12–24 of the N-terminal transmembrane segment of subunit *c* were individually substituted by the large and moderately hydrophobic tryptophan side chain. Effects on the activity of the mutant proteins were studied in selective growth experiments and various ATP synthase specific activity assays. The results identify potential intersubunit contacts and structurally non-distorted, accessible residues in the *c*-oligomer and add constraints to the arrangement of monomers in the oligomeric complex. Results from our mutagenesis experiments were interpreted in structural models of the *c*-oligomer that have been obtained by restrained MD simulations. Different stoichiometries and monomer orientations were applied in these calculations. A cylindrical complex consisting of 10 monomers that are arranged in two concentric rings with the N-terminal helices of the monomers located at the periphery shows the best match with the experimental data.

Keywords: F_1F_0 ATP synthase; Subunit *c*; Oligomer structure; Molecular model

1. Introduction

ATP synthases found in the membranes of eubacteria, mitochondria and chloroplasts catalyse the formation of ATP at the expense of an electrochemical proton gradient. The enzymes are multi-subunit complexes composed of an extramembranous catalytic F_1 domain and a membrane integrated F_0 domain, which translocates protons across the membrane. The transmembrane F_0 domain of the *Escherichia*

Abbreviations: *atpB*, structural gene of the *E. coli* atp operon encoding subunit *a* of the F_1F_0 ATP synthase; *atpE*, structural gene of the *E. coli* atp operon encoding subunit *c* of the F_1F_0 ATP synthase; *atpF*, structural gene of the *E. coli* atp operon encoding subunit *b* of the F_1F_0 ATP synthase; C_{out}, ring-like molecular model of the *c*-oligomer with the C-terminal helices of the monomers located at the peripheral ring; N_{out}, ring-like molecular model of the *c*-oligomer with the N-terminal helices of the monomers located at the peripheral ring

* Corresponding author. Fax: +49-211-8113706;
E-mail: georg.groth@uni-duesseldorf.de

0005-2728/00/$ – see front matter
PII: S0005-2728(00)00112-2

coli enzyme represents the minimal structure of the transmembrane sector of F-ATPases and contains three different polypeptides probably in a stoichiometry of ab_2c_{10-12}. The precise stoichiometry of subunit *c* in the F_0 domain has remained uncertain over the past years. Labelling studies suggested 9–12 copies per complex [1,2]. Recent studies using genetic fusions of subunit *c* clearly favour a stoichiometry of 12 *c*-subunits in the F_0 complex [3]. Studies by Schemidt et al. [4] suggest an adaptable rather than a rigid stoichiometry of *c*-subunits in the F_0 domain depending on the metabolic condition.

The catalytic F_1 domain contains five different polypeptides assembled in a stoichiometry of $\alpha_3\beta_3\gamma\delta\varepsilon$. The structure and the arrangement of subunits in the mitochondrial F_1 domain have been resolved to atomic resolution [5]. The arrangement of subunits in the F_0 domain is not yet resolved to an atomic level. Low resolution structures of the chloroplast and the *E. coli* enzyme obtained by electron microscopy and image analysis suggest that the multiple copies of subunit *c* monomers form a ring-shaped complex in the membrane with subunits *a* and *b* located at the periphery of this oligomeric complex [6–8]. However, a high resolution partial structure of monomeric subunit *c* purified in chloroform:methanol:water was determined by Girvin and Fillingame [9]. The complete structure of the *c*-monomer was solved by heteronuclear NMR techniques, revealing a high resolution structure of the two membrane spanning helices and the connecting hydrophilic loop [10]. Structural changes related to the protonation state of a conserved carboxylate in the C-terminal transmembrane helix were derived from 3D NOESY data [11]. Deprotonation results in a substantial rotation of the C-terminal membrane spanning segment relative to the N-terminal domain. Based on the solvent structure of the protonated and deprotonated *c*-subunit a detailed molecular mechanism for proton translocation and subunit rotation in an ac_{12} complex was proposed by Rastogi and Girvin [11].

Most recently, in the laboratory of J. Walker a structural model of 3.9 Å resolution was determined from crystals of a yeast F_1c_{10} complex which reflects the present resolution limit on the molecular architecture of the transmembrane F_0 sector [12]. Even though the side chain orientation in the ring-shaped *c*-oligomer has not been resolved yet the density map suggests that the N-terminal helices of the *c*-monomers are placed at the inner ring and that the C-terminal membrane spanning domains form the periphery of the oligomer.

A molecular arrangement of subunit *c* in the ring-shaped oligomer has been proposed previously by Groth and Walker [13] on the basis of substitution analysis, chemical, biochemical and genetic data and the high resolution partial structure of the *c*-subunit monomer [9]. Molecular contacts in the oligomeric complex were probed by tryptophan substitution in the C-terminal transmembrane segment of subunit *c* [14] and cysteine crosslinking studies [15]. Different structural models for the arrangement of *c*-subunits in the F_0 complex were deduced from these studies ([13–15], see also [16]). Tryptophan substitution mutagenesis identified residues oriented towards either a helix–helix surface or an accessible phase in the complex and supported the molecular contacts and the arrangement of monomers predicted by Groth and Walker [13]. The constraints on the potential orientation of *c*-subunits in the complex obtained in these studies clearly negate the star-shaped arrangement of monomers that has been proposed from electron microscopic analysis of a 16 kDa polypeptide from V-ATPase with high level of sequence homology to subunit *c* [17,18]. Cysteine crosslinking and modelling studies [15,19] suggest a compact cylindrical structure for the *c*-oligomer which is formed by two concentric rings. In contrast to the model proposed by Groth and Walker [13] the N-terminal helices of the monomers are placed at the centre and the C-terminal helices at the periphery of the oligomer. In addition to the orientation of monomers in the complex, the models differ in the location and the accessibility of the conserved residue *c*D61 which was previously shown to be involved in proton translocation [20]. In the model of Groth and Walker [13] the carboxylate is oriented towards the outside of the oligomeric complex and accessible from the membrane phase as proposed in various theoretical and schematic models for proton transport in the F_0 domain [21–23]. In contrast, the model of Dmitriev et al. [19] places the conserved D61 at the centre of a helical bundle formed by adjacent monomers where it is shielded from the membrane phase.

In order to test the orientation of monomers in the

complex that were proposed by the different models and in order to identify additional contacts and accessible faces in the cylindrical *c*-oligomer, we have extended the tryptophan substitution mutagenesis to the N-terminal segment of subunit *c*. Single tryptophan residues were substituted in positions 12–24 of the N-terminal membrane spanning segment and replacement mutants were studied in a series of ATP synthase specific activity assays. The function of the mutants was disrupted according to a pattern that identified helix–helix contacts and accessible surfaces in the *c*-oligomer and added further constraints to the potential orientation of the monomers in the complex. The results were analysed in the context of a series of molecular models of different subunit stoichiometry and monomer orientation that were obtained by restrained molecular dynamics (MD) simulations [24].

2. Materials and methods

2.1. Strains and vectors

The vector pBWU13 [25] and related derivatives containing tryptophan substitutions in subunit *c* were used for expression of the F_1F_0 ATP synthase in the ATPase deficient strain DK8 of *E. coli* [26]. A derivative of plasmid pMW172 [27] containing a 1211 bp fragment which encodes the entire *atpE* gene and fragments of *atpB* and *atpF* from plasmid pBWU13 was used for the introduction of the tryptophan mutations [14]. Conditions for cell growth and medium composition have been described in detail [14].

2.2. Mutagenesis of subunit c

The pMW172 derivative containing the *atpE* gene encoding subunit *c* was used as a template for introducing mutations by sequential PCR amplification as described [14]. The amplified fragments were agarose gel purified using the QIA-quick gel extraction kit (Qiagen, Hilden, Germany), digested with *Pfl*MI and *Ppu*MI and ligated into the equivalent site of plasmid pWBU13 which was predigested with the same restriction enzymes. The inserted fragments were sequenced using a series of primers complementary to both strands of *atpE*, *atpB* and *atpF* to verify the targeted mutation and the absence of accidentally introduced additional mutations by the polymerase.

2.3. Isolation of membrane vesicles

Cells of strain DK8 were transformed with plasmid pBWU13 or derivatives encoding the mutated or wild type form of the F_1F_0 ATPase. Plasmid pBR322 was used as a control for cells with no endogenous ATPase activity. Single colonies were picked and grown in 2YT medium containing 0.5% (w/v) glucose. At an OD_{578} of 1.4–1.6 cells were harvested by centrifugation at $5000 \times g$ for 10 min at 4°C. Cell pellets were resuspended in ice-cold medium containing 50 mM Tricine (pH 8.0), 10 mM $MgCl_2$ and 10% (v/v) glycerol to a density of 0.3 g cells/ml of medium. Afterwards cells were disrupted by sonication as described elsewhere [28] and centrifuged at $30\,000 \times g$ for 10 min to separate cellular debris from membrane vesicles. Membrane vesicles were collected by centrifuging the resulting supernatant at $250\,000 \times g$ for 75 min at 4°C. The pelleted membrane vesicles were resuspended in 0.4 ml medium. The protein content of the membrane preparation was determined by the bicinchoninic acid assay (Pierce Chemicals, Rockford, IL, USA) using bovine serum albumin as a standard. Stocks of the membrane vesicles were kept on ice for activity measurements.

2.4. Screening for growth on succinate minimal medium

A minimal medium according to Tanaka et al. [29] containing 50 μg/ml thymine, 2 μg/ml thiamine, 50 μg/ml asparagine, leucine and valine and 0.5% (w/v) succinate as carbon source was used to test whether cells containing the mutant proteins still have a functional oxidative phosphorylation and an intact ATPase. Wild type, control or mutant plasmids were transferred into strain DK8 and grown in LB medium for 60 min. Cells were precipitated at $1500 \times g$, resuspended in 10 mM Tris–HCl pH 8.0 and plated on minimal medium. Plates were incubated at 37°C for 2–3 days.

2.5. Measurement of F_1F_0 ATP synthase activity

The ATPase activity of wild type and mutant membrane vesicles was monitored in a medium containing 20 mM Tricine pH 8.0, 150 mM KCl, 5 mM $MgCl_2$, 1 μM nigericin and 0.3 mg/ml membrane protein. The reaction was started by adding 2 mM ATP to the reaction medium preincubated at 25°C. At regular intervals 0.15 ml aliquots were withdrawn and the ATPase activity in the samples was quenched by the addition of 1 M trichloroacetic acid. Phosphate release in the samples was determined according to Taussky and Shorr [30] in a spectrophotometric assay.

Proton translocation in the membrane vesicles caused by NADH oxidation or ATP hydrolysis was detected by fluorescence quenching of 9-amino-3-chloro-7-methoxyacridine. Vesicles were incubated at 25°C in the same reaction medium used in the ATPase assay but lacking the nigericin. Quenching was initiated by the addition of 1 mM ATP or 0.3 mM NADH to the reaction medium containing 0.1 mg/ml membrane protein and 0.25 μM of the acridine dye. Non-specific quenching caused by the interaction of free fluorescent dye and ATP was determined at the end of the assay by adding 1 μM nigericin to the medium.

2.6. Immunodetection of the c-subunit

Expression and membrane insertion of subunit *c* in cells carrying the mutations was compared to wild type cells by SDS–PAGE and Western blotting. Plasmid pBR322 was used as a control for cells lacking F_1F_0 subunits. Equal amounts of membrane vesicles prepared from mutant, wild type and control cells were loaded onto an SDS gel containing 15% polyacrylamide. The separated proteins were transferred onto a polyvinylidene difluoride membrane (Millipore, Bedford, MA, USA) by a Pharmacia Multiphor II semidry blotting system. Protein transfer was examined by reversible Ponceau S staining. The unspecific binding capacity of the membrane was blocked with 1% (w/v) casein in TBS-T buffer containing 50 mM Tris pH 7.4, 152 mM NaCl and 0.05% (v/v) Tween 20. All further washing steps were performed in TBS-T buffer. The anti-*c* polyclonal antibody (kindly provided by I. Arachaga, MRC Laboratory of Molecular Biology, Cambridge, UK) and the secondary antibody coupled to horseradish peroxidase were diluted 1:5000 and 1:15 000, respectively, in TBS buffer. Detection of subunit *c* was carried out using BM Chemiluminescence Western blotting reagents (Boehringer Mannheim, Mannheim, Germany).

2.7. Prediction of steric conflicts in the c-subunit oligomer caused by tryptophan substitution

Contacts and steric conflicts between side chains or backbone atoms in adjacent monomers caused by the substitution of tryptophan residues in positions 12–24 of the N-terminal membrane spanning segment were calculated by the software Swiss-PdB-Viewer [31] on the basis of the co-ordinates from various molecular models of the *c*-oligomer that have been obtained in restrained MD simulations. The calculation of the best rotamer for the introduced tryptophan residues has been described by Groth et al. and Guex and Peitsch [14,31]. Details of the modelling and simulations have been reported by Forrest et al. [24]. Calculation of solvent accessible area was carried out using Xplor [32].

3. Results

3.1. Growth on minimal medium

Growth of colonies on succinate minimal medium was taken as indicative of a functional oxidative phosphorylation system and an intact ATP synthase in the mutant cells. Strain DK8 was transformed with control plasmid pBR322, plasmid pBWU13 or

Table 1
Cell growth of substitution mutants on succinate minimal medium

Mutant	WT	A12W	A13W	A14W	V15W	M16W	M17W	G18W	L19W	A20W	A21W	I22W	G23W	A24W
Growth	+	+	−	+	+	+	+	−	+	−	−	+	−	−

its mutant derivatives and plated on minimal medium. Growth of colonies on plates that were incubated at 37°C for 2–3 days was taken as initial evidence that mutant cells still contain a functional ATP synthase with no extensive structural disruption in the membrane spanning domain caused by the tryptophan substitution. The results of these screening experiments are summarised in Table 1. Colonies were only detected in the case of the wild type and when residues 12, 14, 15, 16, 17, 19 or 22 in the N-terminal transmembrane domain of subunit *c* were substituted by tryptophan. Host cells transformed with the control plasmid and plasmids carrying substitutions in position 13, 18, 20, 21, 23 or 24 of subunit *c* showed no growth of colonies on the minimal medium plates.

3.2. ATP driven proton translocation

Detection of proton translocation across the F_0 domain represents a sensitive assay to test the structural integrity of the membrane spanning domain of the ATP synthase after tryptophan substitution. Extents of proton gradients formed at the expense of ATP hydrolysis in the F_1 domain were monitored by fluorescence quenching of a sensitive acridine dye. The relative extents of the transmembrane proton gradients formed in the various substitution mutants of subunit *c* are summarised in Fig. 1A. Minor effects on proton translocation were found for replacement mutants *c*V15W, *c*L19W and *c*I22W which showed 80–90% of the wild type activity. Decreased rates of about 70 and 50%, respectively, were detected when membrane vesicles of mutants with substitutions in position 16 or 17 of the *c*-subunit were tested. A significantly decreased activity of 5–7% was observed for mutants *c*A12W and *c*A14W, which is only slightly above the background level detected in the controls. Membranes of mutants *c*A13W, *c*G18W, *c*A20W, *c*A21W, *c*G23W and *c*A24W showed no ATP induced proton translocation in the activity assays, which suggests a substantial distortion or disruption in the membrane spanning *c*-oligomer of these mutants. In order to test whether reduced proton gradients observed by the acridine quenching are related to a non-functional ATP synthase and an impaired F_0 domain rather than an enhanced non-specific proton permeability of the mutant membranes, the generation of a proton gradient at the expense of NADH was also monitored in the mutant membrane vesicles. However, no significant decrease in the transmembrane gradient compared to wild type cells was detected for any of the replacement mutants (data not shown).

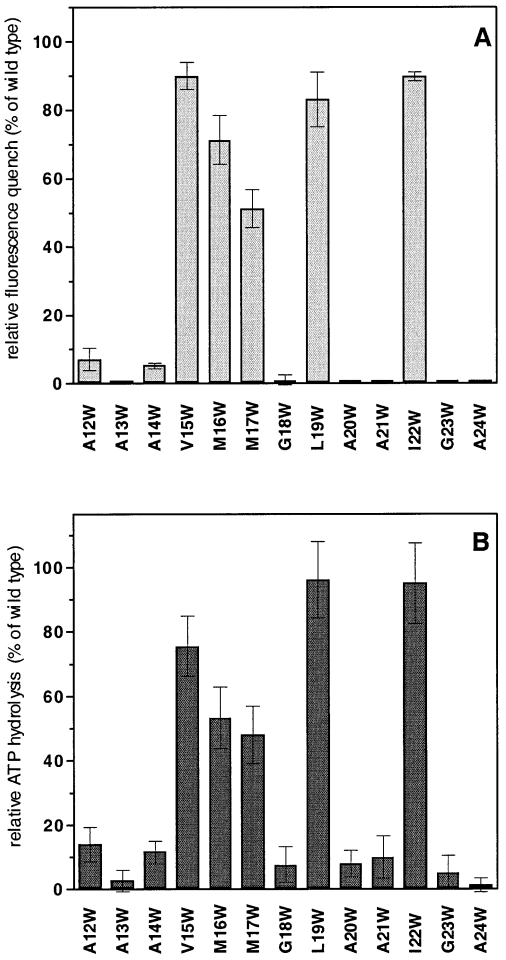

Fig. 1. Effects of tryptophan substitution in the N-terminal domain of subunit *c* on ATP dependent proton translocation and ATP hydrolysis. (A) Quenching of the acridine dye 9-amino-3-chloro-7-methoxyacridine on addition of 2 mM ATP in mutant membrane vesicles. Signals were recorded at $\lambda_{em} = 490$ nm and are related to the maximal extent of quenching observed with the wild type. (B) ATPase activity in membrane vesicles of replacement mutants. Rates of ATP hydrolysis were related to the maximal activity of 0.1 μmol mg^{-1} min^{-1} determined for the wild type enzyme.

3.3. ATPase activity of tryptophan replacement mutants

A disruption or distortion of the transmembrane F_0 domain caused by the incorporation of tryptophan residues into subunit *c* probably also affects the association of and the interaction between the extramembranous F_1 and the membrane integrated F_0 sectors. Differences in ATP hydrolysis observed in membrane vesicles of mutant and wild type enzymes are, therefore, indicative of altered interactions between the domains as well as conflicts in the membrane spanning F_0 complex. Relative rates of membrane bound ATP hydrolysis observed for mutant membrane vesicles are given in Fig. 1B for replacement mutants in positions 12–24 of subunit *c*. Activities corresponding to the wild type enzyme were found when valine 15, leucine 19 or isoleucine 22 were replaced by tryptophan. Reduced ATPase activities were obtained for mutants *c*M16W and *c*M17W, which showed about 50% of the wild type level. Hydrolysis rates of mutants *c*A12W, *c*A14W and *c*A21W were reduced to 10–15% of the wild type activity. Activities below 10%, which might reflect an unspecific, intrinsic activity of the assay, were detected when membrane vesicles of mutants *c*A13W, *c*G18W, *c*A20W, *c*A23W or *c*A24W were tested.

3.4. Immunodetection of subunit c in wild type and replacement mutants

In order to test whether the mutant *c*-subunits were stable and properly inserted into the plasma membrane, wild type and mutant membrane vesicles were analysed by SDS–PAGE and immunoblotting. The Western blot in Fig. 2 shows that a band corresponding to the *c*-subunit monomer with an apparent molecular mass of 6.5 kDa was observed for all mutant proteins. The expression of the mutant proteins seems to be comparable to the wild type level and their targeting to the plasma membrane appears not to be affected by the tryptophan substitutions. No signal was detected when the control plasmid pBR322 was transferred to the ATPase deficient strain DK8 (see Fig. 2, lanes 2 and 16). The Western blot analysis of the mutant membrane vesicles clearly demonstrates that any effects observed in screening experiments and activity assays are related to a non-functional oligomer structure rather than unstable or non-expressed subunit *c* monomers.

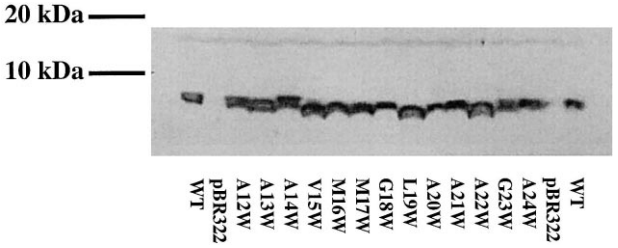

Fig. 2. Immunoblot analysis of N-terminal tryptophan replacement mutants. Membrane vesicles of wild type (lanes 1 and 17), ATP synthase deficient control (lanes 2 and 16) and tryptophan replacement mutants (lanes 3–15) were resolved on a 15% polyacrylamide gel, blotted on a polyvinylidene difluoride membrane and probed with an anti-*c* polyclonal antibody. Molecular masses of marker proteins are given on the left side in kDa.

3.5. Prediction of contacts and steric conflicts in the c-oligomer

Effects of tryptophan substitution in positions 12–24 of the N-terminal membrane spanning segment of subunit *c* on the intermolecular contacts of adjacent monomers in the oligomeric complex were predicted by the macromolecular modelling software Swiss-PDB-Viewer [31]. Molecular models obtained by restrained MD simulations for oligomers formed of 9, 10 or 12 subunit *c* monomers [24] were applied in these calculations. In addition to variation in stoichiometry, the orientation of the monomers in the oligomeric complex was varied, and models placing either the N- or the C-terminal transmembrane helices at the periphery of the complex were constructed in these studies. Models with the N-terminal helices located at the periphery in the oligomer were calculated based on the molecular model of Groth and Walker [13]. Models with an external orientation of the C-terminal helices in the complex were constructed from these models by assumption of symmetry (for details see [24]). The most symmetrical model showing the smallest RMSD variation of the 25 models calculated for each stoichiometry and monomer orientation in the restrained MD simulations was selected and residues in positions 12–24 were substituted by tryptophan. The average score for the substitution in a certain position is given in

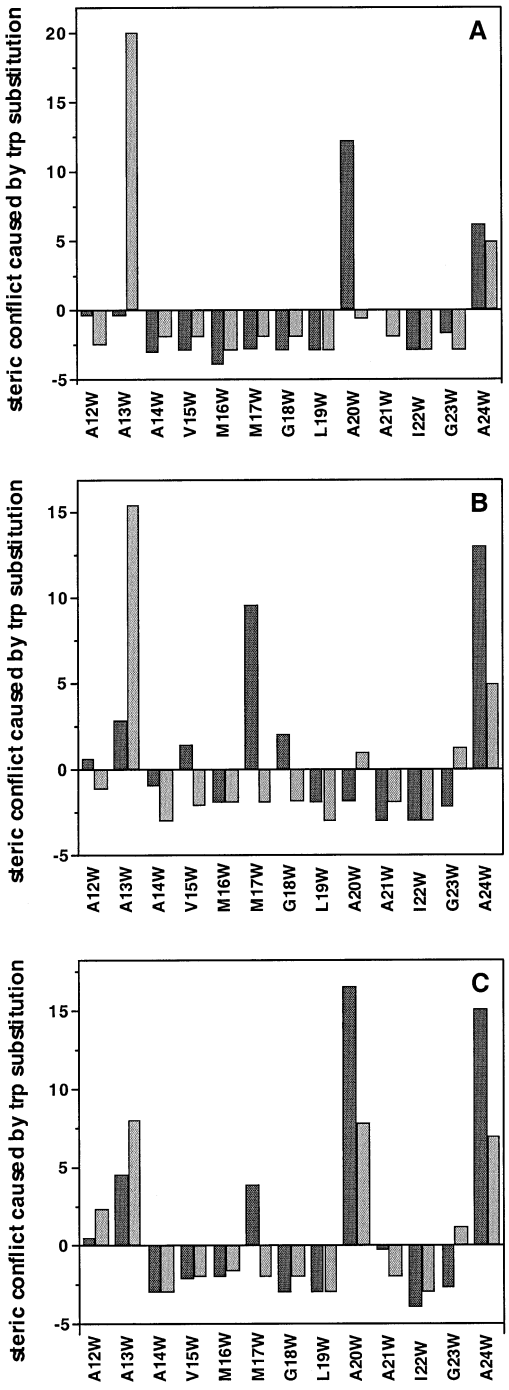

Fig. 3A–C which compares the calculations for models with stoichiometries of 9, 10 and 12 monomers per complex that differ in the location of the N-terminal or the C-terminal helix, respectively. The score numbers reflect the best conformation of the tryptophan side chain in the complex with minimal internal

Fig. 3. Prediction of contacts and steric conflicts in the *c*-oligomer for replacement mutants in position 12–24 of the N-terminal membrane spanning segment. Steric conflicts were calculated on the basis of structural data from molecular models obtained by restrained MD simulations [24] by the modelling software Swiss-PDB-Viewer [31]. Positive numbers indicate inter- or intramolecular conflicts with the backbone or side chains of adjacent monomers that are expected to distort or disrupt the oligomer structure and result in non functional mutants. (A) Oligomer consisting of nine *c*-subunits. (B) Complex formed of 10 monomers. (C) Dodecameric complex with either C_{out} (dark grey) or N_{out} (light grey) orientation of the membrane spanning helices of subunit *c*.
←

constraints selected from a collection of acceptable conformations. On the basis of these numbers intact and distorted structures in the replacement mutants are discriminated. Positive numbers indicate steric conflicts caused by intra- or intermolecular contacts. Negative numbers suggest that no structural conflict is expected in the oligomer. Different predictions for the two orientations of the monomers may enable prediction of the correct orientation of the monomers when correlated to the experimental results.

As shown in Fig. 3A most tryptophan substitutions are expected to be tolerated in a complex formed of nine *c*-subunits. The predictions for the two different monomer orientations in the complex (N_{out} and C_{out}) differ only for substitutions in position 13 and 20. Differences become more evident in a complex formed by 10 monomers shown in Fig. 3B. In these structural models substitutions in eight positions of the N-terminal helix are expected to cause distortion of the oligomer resulting in non-functional mutant proteins. Different predictions of structural conflicts between the N_{out} and the C_{out} models are obtained for residues 12, 15, 17, 18, 20 and 23. The N_{out} model is predicted to have a functional F_0 domain for replacement mutants *c*A12W, *c*V15W, *c*M17W and *c*G18W. The C_{out} model assumes steric conflicts for tryptophan substitutions in these positions but predicts functional enzymes for mutants *c*A20W and *c*G23W. In a dodecamer, different predictions are obtained for the N_{out} versus the C_{out} model for the substitution of methionine 17 and glycine 23 (see Fig. 3C). A non-functional mutant is expected for replacement mutant *c*G23W in the N_{out} model. The C_{out} model predicts steric conflicts for the substitution of methionine 17 by tryptophan.

4. Discussion

The arrangement of subunit *c* monomers in the membrane domain of F_1F_0 ATPases has been studied by image analysis, chemical modification and scanning mutagenesis in the past [14,15, 17,18,33]. Experimental data were interpreted in molecular models of the oligomeric subunit *c* complex that show substantial differences in stoichiometry, arrangement and orientation of monomers in the complex. Star-shaped [17,18] or ring-like [14,15] models of the *c*-oligomer were proposed placing either the N-terminal or the C-terminal helices of the monomers in the centre of the complex. In the work presented here, new constraints on arrangement and orientation of monomers in the oligomeric complex are obtained from tryptophan scanning mutagenesis studies in the N-terminal transmembrane segment of subunit *c*. These extend previous substitution experiments in the C-terminal membrane spanning segment [14]. In these studies tryptophan residues were substituted in consecutive positions in subunit *c*. The large and hydrophobic tryptophan residue should be tolerated only at an external or internal surface in the oligomer. Placing the side chain at the interacting surface of adjacent monomers should disrupt the structure and affect protein function. ATP synthase specific activity assays and screening experiments on minimal medium which are indicative of a functional ATPase suggest that mutations in positions 12–14, 18, 20, 21, 23 and 24 of the N-terminal transmembrane helix cause steric conflicts in the oligomer resulting in a non-functional ATPase. Substitutions in positions 15–17, 19 and 22 show no or only moderate effects on the activity of the enzyme (see Fig. 1A,B) and suggest that these positions are not involved in intermolecular contacts in the complex.

Results from screening experiments and activity assays are consistent. However, growth of mutants *c*A12W and *c*A14W on minimal medium and the extremely low activity of these mutants found in ATP hydrolysis and ATP driven proton translocation indicate that activity assays may provide a more sensitive analysis.

Theoretical calculations of steric conflicts caused by the introduction of tryptophan residues were compared to the experimental results described in this work in six different cylindrical models of the *c*-oligomer [24] in order to discriminate the relative orientation of monomers in the oligomeric complex. In a complex formed by nine monomers, several differences between theoretical prediction and activity measurement are evident for both orientations (see Figs. 1 and 3A). The models propose functional enzymes for most substitutions which are not consistent with the experimental data obtained for the inactive mutants *c*A14W, *c*G18W, *c*A21W and *c*G23W. Hence, no obvious distinction between a C_{out} or a N_{out} orientation of the monomers is evident for a complex which contains nine *c*-subunits.

Models with 10 monomers in the complex predict steric conflicts for several positions in the N-terminal transmembrane segment after tryptophan substitution. The N_{out} model reflects the results obtained in activity measurements for most replacement mutants except substitutions *c*G18W and *c*A21W. Both substitutions show no functional ATPase in the activity assays whereas the calculations reveal no steric distortion in the complex. However, functional rather than structural reasons might cause the non-functional mutants, i.e. effects on the transient interaction with subunit *a* at the periphery of the *c*-oligomer that might distort the proposed relative rotation of subunits *a* and *c* during the catalytic mechanism. Visual examination of the models reveals that the tryptophan mutant residues in *c*G18W do indeed lie on the periphery of the oligomer and may conceivably result in disruption of the *a* to *c* interaction. For replacement mutant *c*A21W the model suggests a potential interaction with the essential *c*D61 that might affect protonation during the catalytic turnover.

The structural model of 10 monomers which contains the C-terminal helices at the periphery of the complex (C_{out}) is less consistent with the experimental data. Structural distortions in the oligomer that are predicted for substitution of residues valine 15 and methionine 17 disagree with the results from replacement mutants *c*V15W and *c*M17W which show high activity in ATP hydrolysis and ATP driven proton translocation. Functional mutants predicted for substitutions in positions 20 and 23 also contradict experimental data obtained with these mu-

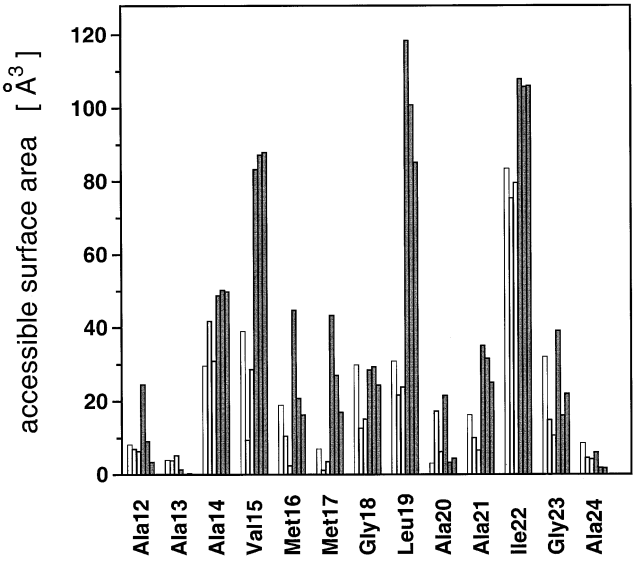

Fig. 4. Accessible surface area of residues in the N-terminal membrane spanning segment in different structural models of the *c*-oligomer obtained by restrained MD simulations (22). Calculations are shown only for positions that were substituted by tryptophan in the mutagenesis study presented in this work. (□) Calculations for C_{out} models with 9, 10 or 12 monomers; (■) calculations for N_{out} models with 9, 10 or 12 monomers in the complex.

tants. In contrast to the N_{out} model, however, the disruptive effect of mutation *c*G18W, as predicted by the C_{out} model, reflects the experimental data.

Theoretical predictions and experimental results from replacement mutants *c*A12W, *c*G18W and *c*A21W disagree for both monomer orientations in the dodecameric models. Different orientational effects, however, are predicted for the substitution of methionine 17 and glycine 23 in the dodecamer. In both cases, the predictions made by the N_{out} model correspond to the experimental data (see Figs. 1 and 3C), but calculations from the C_{out} model are in contradiction to these results.

The location of the N-terminal helices at the external side of the oligomeric *c*-cylinder is also supported by the calculated accessible surface area of residues in the N-terminal transmembrane segment which are summarised in Fig. 4 for the various models. Residues valine 15, methionine 16, methionine 17, leucine 19 and isoleucine 22 which correspond to functional substitution mutants have significantly higher accessible surface areas in all three oligomer states in the N_{out} models than in the C_{out} models.

Further evidence on the orientation of the monomers in the *c*-subunit oligomer comes from labelling studies using the hydrophobic membrane penetrating probe TID [33]. In functional F_0 only residues exposed to the membrane phase are modified. Analysis of the residues modified by the carbene in the different structural models of the *c*-oligomer reveals that in the case of the N_{out} orientation of the monomers the labelled residues form a more or less continuous surface at the outside of the *c*-cylinder and are exposed and accessible from the lipid phase. In the C_{out} orientation these residues are located at the interior of the pore formed by the cylindrical complex. While the N_{out} models reflect the labelling pattern which is expected for a lipophilic probe distributed in the membrane as only residues on the external side of the complex are modified, the pattern in the C_{out} models is less evident. Even by assuming that the probe can diffuse into the centre of the cylindrical complex and distribute in a potential lipid phase inside the oligomer, it seems obscure why almost no residue at the outside, lipid exposed surface of the cylinder is modified in the C_{out} orientation.

Immunolabelling also seems to support the location of the N-terminal helices at the periphery of the *c*-oligomer. Binding of peptide specific antibodies directed against the region around *c*K34–*c*R41 is observed for F_1F_0 as well as for isolated F_0 [34]. The related antigenic epitope is accessible from the outside in the N_{out} models, but located at the inside of the oligomer in the C_{out} models. In particular with the globular F_1 complex attached to the F_0 domain the binding of the antibody to the epitope is difficult to reconcile. A peripheral location of the epitope in the cylindrical *c*-oligomer as in the N_{out} models, however, would probably not affect the binding of the specific antibody to the F_1F_0 complex.

In contrast, disulphide crosslinking studies from B. Fillingame's laboratory suggest a peripheral location of the C-terminal helices in the oligomeric *c*-subunit complex [35,36]. The most compelling evidence for a C_{out} orientation in the oligomer appear to be the disulphide crosslinks of residues *c*A62C, *c*M65C, *c*G69C, *c*L72C and *c*Y73C with subunit *a* [35]. The observed crosslink products, however, are also consistent with an N_{out} orientation in the complex as most of these residues pack into the gap between

adjacent helices in the outer concentric ring of the oligomer. Substitution of cysteine residues in the related positions of the C-terminal membrane spanning helix showed that sulphur atoms are still accessible from the outside of the cylinder in the N_{out} models (data not shown). Thus the formation of disulphides with cysteine residues in subunit *a* seems possible in particular when some flexibility and mobility of the transmembrane helices in the F_0 domain is considered. Such flexibility and reorientation of the membrane spanning helices during catalytic turnover is suggested from the structural changes which were found in the protonated and deprotonated form of solvent purified subunit *c* [11].

Current schematic models on proton translocation and energy transduction in the transmembrane F_0 domain [21–23] assume a direct interaction of the conserved aspartate 61 in subunit *c* with residues in subunit *a* which is probably located at the outside of the *c*-oligomer [6]. In the structural model proposed by Groth and Walker [13] and the related new models obtained by restrained MD simulations [24] carboxyl oxygens of the conserved *c*D61 are accessible from the external side of the cylindrical complexes. Exposure of aspartate 61 is substantially higher in the C_{out} models, but N_{out} models also show adequate access to the carboxylate. Thus transient contacts of *c*D61 and *a*R210 during proton translocation across the transmembrane F_0 domain that have been suggested from mutagenesis studies [37] seem possible in these structures.

In the model presented by Dmitriev et al. ([19], see also [15]), where the C-terminal membrane spanning segment is located at the periphery of a compact cylinder formed by back-to-front packed *c*-monomers, the carboxylate of *c*D61 is shielded by the back of the transmembrane helix and buried in the helical bundle formed by adjacent monomers. Hence interaction with *a*R210 would require substantial reorientation of adjacent *c*-monomers such as opening and closing of the helical bundle which is suggested to form the functional unit in the oligomer. Such a rotation and swivelling of adjacent monomers during the catalytic turnover, however, seems questionable on the basis of functional disulphide crosslinks formed in the C-terminal helix [36]. Mutations *c*I66C, *c*V74C, *c*M75C and *c*V78C which were shown to form high yield crosslink products should clamp adjacent C-terminal helices in the bundle and block the crucial rotation of about 120° to allow access to *c*D61 buried in the bundle of adjacent monomers. Consequently no activity should be associated with these mutations. Experimental data, however, show that growth properties of these mutants on minimal medium resemble the wild type [36]. Thus the aspartate must still be accessible in these crosslinked products in the absence of rotation or reorientation of the helices.

A less compact arrangement of the *c*-monomers in the oligomer as suggested by Dmitriev et al. [19] was calculated from the structural data of the protonated and deprotonated *c*-subunit by dynamics simulated annealing [11]. In contrast to the C_{out} model of the dodecamer presented in this work the deprotonated form of subunit *c* was taken for the monomer contacting subunit *a*, while the remaining monomers in the dodecamer were assumed to exist in their protonated state. Based on this model a detailed molecular mechanism was proposed that links proton translocation to a rotation of the *c*-oligomer with respect to the static *a* subunit. Access to the conserved carboxylate *c*D61 was attributed to hydrophilic pathways formed by polar residues in subunit *a* (for details see [11]). However, it is questionable whether this attractive model reflects the general mechanism of proton transport and subunit rotation in the F_0 domain as polar residues *a*N148, *a*D119, *a*H245, *a*S144 and *a*N238 which are supposed to form a hydrophilic path connecting *c*D61 to the periplasmic membrane surface in *E. coli* are not conserved amongst ATP synthases. Moreover, the alignment of water molecules in the predicted channels at the contact face between subunits *a* and *c* seems problematic in the context of a rotation of the *c*-ring against the *a*-subunit in the hydrophobic membrane phase. In addition experimental data from Trp replacement studies presented in this work are not in agreement with the suggested arrangement of monomers in the model which predicts steric conflicts for the functional substitution mutants *c*M16W, *c*M17W and *c*L19W and a functional F_0 complex in the distorted mutant *c*A21W.

In summary, the substitution mutagenesis study presented in this work somewhat favours a peripheral location of the N-terminal helices in the *c*-oligomer of the bacterial ATPase as suggested [13,14].

However, it should be emphasised that models never substitute for a high resolution structure. Thus, the most compelling evidence for an external location of the C-terminal helices in the transmembrane *c*-oligomer comes from very recent data on the yeast ATP synthase [12]. The 3.9 Å structure map obtained from crystals of a F_1c_{10} complex of the yeast enzyme indicate a kink in the helices that are located at the periphery of the ring. Even though the sequence homology of the yeast and the *E. coli* *c*-subunit is rather low the kink and the continuous electron density found for both transmembrane helices seem to support that the C-terminal helices of the *c*-subunit form the outer ring in the *c*-oligomer. Nevertheless, results from Trp substitution ([14], this work) and TID and immunolabelling studies are difficult to reconcile with such an arrangement of the monomers in the ring.

The present contradictions might be resolved either by a molecular structure of the yeast F_1c_{10} complex at atomic resolution, by labelling studies of the yeast ATP synthase or by studying the location of tryptophan residues in the isolated F_1F_0 complex of different substitution mutants by native gel electrophoresis or fluorescence spectroscopic techniques. Preliminary fluorescence experiments have demonstrated that intrinsic Trp residues in subunits α, β, γ, δ, *a* and *b* must be removed before the orientation of the tryptophan residues in subunit *c* and thereby the location of the helices in the cylindrical oligomer can be resolved. Plasmids encoding Trp reduced ATP synthase kindly provided by S. Wilke-Mounts and A. Senior are now used to construct these Trp substitution mutants in subunit *c*. In addition these studies may allow the monitoring of the dynamic protein–protein interactions in the F_0 domain that occur during the catalytic reaction.

Acknowledgements

This work was supported through the Deutsche Forschungsgemeinschaft SFB 189. L.R.F. is an MRC student and the work in M.S.P.S.'s lab is supported by the Wellcome Trust.

References

[1] D.L. Foster, R.H. Fillingame, J. Biol. Chem. 257 (1982) 2009–2015.
[2] K. von Meyenburg, B.B. Jørgensen, J. Nielsen, F.G. Hansen, O. Michelsen, Tokai J. Exp. Clin. Med. 7 (1982) 23–31.
[3] P.C. Jones, R.H. Filligame, J. Biol. Chem. 273 (1998) 29701–29705.
[4] R.A. Schemidt, J. Qu, J.R. Williams, W.S. Brusilow, J. Bacteriol. 180 (1998) 3205–3208.
[5] J.P. Abrahams, A.G.W. Leslie, R. Lutter, J.E. Walker, Nature 370 (1994) 621–628.
[6] R. Birkenhäger, M. Hoppert, G. Deckers-Hebestreit, F. Mayer, K. Altendorf, Eur. J. Biochem. 230 (1995) 58–67.
[7] S. Singh, P. Turina, C.J. Bustamante, D.J. Keller, R. Capaldi, FEBS Lett. 397 (1996) 30–34.
[8] D. Neff, S. Tripathi, K. Middendorf, H. Stahlberg, H.J. Butt, E. Bamberg, N.A. Dencher, J. Struct. Biol. 119 (1997) 139–148.
[9] M. Girvin, R. Fillingame, Biochemistry 34 (1995) 1635–1645.
[10] M.E. Girvin, V.K. Rastogi, F. Abildgaard, J.L. Markley, R.H. Fillingame, Biochemistry 37 (1998) 8817–8824.
[11] V.K. Rastogi, M.E. Girvin, Nature 402 (1999) 263–268.
[12] D. Stock, A. Leslie, J.E. Walker, Science 268 (1999) 1700–1704.
[13] G. Groth, J.E. Walker, FEBS Lett. 410 (1997) 117–123.
[14] G. Groth, Y. Tilg, K. Schirwitz, J. Mol. Biol. 281 (1998) 49–59.
[15] P. Jones, W. Jiang, R.H. Fillingame, J. Biol. Chem. 273 (1998) 7178–17185.
[16] G. Groth, Biochim. Biophys. Acta (2000) in press.
[17] M.E. Finbow, E.E. Eliopolous, P.J. Jackson, J.N. Keen, L. Meagher, P. Thompson, P.C. Jones, J.B.C. Findlay, Protein Eng. 5 (1992) 7–15.
[18] A. Holzenburg, P.C. Jones, T. Franklin, T. Pali, T. Heimburg, D. Marsh, J.B.C. Findlay, M.E. Finbow, Eur. J. Biochem. 213 (1993) 21–30.
[19] O.Y. Dmitriev, P.C. Jones, R.H. Fillingame, Proc. Natl. Acad. Sci. USA 96 (1999) 7785–7790.
[20] M.J. Miller, M. Oldenburg, R.H. Fillingame, Proc. Natl. Acad. Sci. USA 87 (1990) 4900–4904.
[21] W. Junge, D. Sabbert, S. Engelbrecht, Ber. Bunsenges. Phys. Chem. 100 (1996) 2014–2019.
[22] T. Elston, H. Wang, G. Oster, Nature 391 (1998) 510–513.
[23] S.B. Vik, B.J. Antonio, J. Biol. Chem. 269 (1994) 30364–30369.
[24] L.R. Forrest, G. Groth, M.S.P. Sansom, (1999). Submitted to Biophys. J.
[25] Y. Moriyama, A. Iwamoto, H. Hanada, M. Maeda, M. Futai, J. Biol. Chem. 266 (1991) 22141–22146.
[26] D.J. Klionsky, W.S. Brusilow, R.D. Simoni, J. Bacteriol. 160 (1984) 1055–1060.

[27] M. Way, B. Pope, J. Gooch, M. Hawkins, A.G. Weeds, EMBO J. 9 (1990) 4103–4109.
[28] K. Steffens, E. Schneider, G. Deckers-Hebestreit, K. Altendorf, J. Biol. Chem. 262 (1987) 5866–5869.
[29] S. Tanaka, S.A. Lerner, E.C. Lin, J. Bacteriol. 93 (1967) 642–648.
[30] H.H. Taussky, E. Shorr, J. Biol. Chem. 202 (1953) 675–685.
[31] N. Guex, M.C. Peitsch, Protein Data Bank Q. Newslett. 77 (1996) 7.
[32] A.T. Brünger, X-PLOR Version 3.1. A System for X-ray Crystallography and NMR, Yale University Press, New Haven, CT, 1992.
[33] J. Hoppe, W. Sebald, Biochim. Biophys. Acta 768 (1984) 1–27.
[34] M. Hensel, G. Deckers-Hebestreit, R. Schmidt, K. Altendorf, Biochim. Biophys. Acta 1016 (1990) 63–70.
[35] W. Jiang, R.H. Fillingame, Proc. Natl. Acad. Sci. USA 95 (1998) 6607–6612.
[36] P. Jones, W. Jiang, R.H. Fillingame, J. Biol. Chem. 273 (1998) 17178–17185.
[37] D. Fraga, J. Hermolin, R.H. Fillingame, J. Biol. Chem. 269 (1994) 2562–2567.